ELSEVIER

Journal of Photochemistry and Photobiology A: Chemistry 133 (2000) 45–50

Journal of Photochemistry and Photobiology A:Chemistry

www.elsevier.nl/locate/jphotochem

Laser flash photolysis study on photophysical and photochemical properties of C_{60} fine particles

Mamoru Fujitsuka [a], Hitoshi Kasai [a], Akito Masuhara [a], Shuji Okada [a], Hidetoshi Oikawa [a], Hachiro Nakanishi [a], Osamu Ito [a,*], Kiyoshi Yase [b]

[a] *Institute for Chemical Reaction Science, Tohoku University, Katahira, Sendai 980-8577, Japan*

[b] *National Institute of Materials and Chemical Research, 1-1 Higashi, Tsukuba, Ibaraki 305-8565, Japan*

Received 21 October 1999; received in revised form 15 December 1999; accepted 18 January 2000

Abstract

Photophysical and photochemical properties of the C_{60} fine particles (C_{60}FP) which were prepared by the reprecipitation method were examined by the time-resolved fluorescence and laser flash photolysis methods. Fluorescence decay of the fine particles can be divided into two components: emission from free exciton and self-trapped exciton. Rapid decay of the broad absorption after nanosecond-laser excitation was attributed to triplet–triplet annihilation due to migration of energy of triplet state within the fine particle. After the annihilation, the energy of triplet state localized on C_{60} molecule. Energy transfer from the localized C_{60} triplet state in the fine particle was confirmed for energy acceptors such as O_2 and β-carotene. Photoexcitation of the C_{60}FP in the presence of electron donor in solution resulted in photoinduced electron transfer. The reaction rate constant was one order smaller than that in solution, suggesting small collision frequency of the localized triplet state in C_{60}FP. Oxidation of the fine particle was also observed by using methylacridinuim ion and biphenyl as a sensitizer and a cosensitizer, respectively.

Keywords: Fine particle; Fullerene; Photoinduced electron transfer

1. Introduction

Fine particle or microcrystal with nanometer-order diameter attracts a lot of interest because of its size-dependent properties such as confinement effect (for example [1]). These interesting properties have been investigated for understanding the basic physical and chemical phenomena and for the application to non-linear optics of fine particle [2]. Furthermore, chemical reactivity of these fine particles are much higher than bulk materials due to its wide surface area. While almost these investigations have been made on inorganic semiconductors and metallic materials, organic molecule can also be regarded as a promising candidate for interesting materials. Recently, organic fine particles have been prepared by several methods: reprecipitation method [3,4], evaporation method [5], and so on [6].

Fullerenes are also considered to be one of the candidates for organic fine particles with interesting properties. Fullerenes are reported to form aggregates in poor solvents [7–9]. Generation mechanism of the aggregates has been discussed based on the results of several experimental techniques such as dynamic light scattering. The dimension of these aggregates varies from about 100 to 1000 nm depending on several experimental conditions such as concentration. The laser flash photolysis study shows that the photophysical and photochemical properties of C_{60} solution are sensitive to the formation of C_{60} aggregates.

In the present paper, we have prepared well-controlled C_{60} fine particles (C_{60}FP) by the reprecipitation method for better understanding of the photophysical and photochemical properties of these fine particles. Its structural information was obtained by transmission electron microscopy (TEM), electron diffraction, and dynamic light scattering methods. For C_{60}FP dispersion in ethanol, photophysical and photochemical properties were examined by several time-resolved spectroscopies such as nanosecond-laser flash photolysis.

2. Experimental

2.1. Materials

C_{60} (99.5%) was purchased from Term Co. *N*-Methylacridinium hexafluorophosphate (NMA^+) was synthesized

* Corresponding author. Fax: +81-22-217-5610.
E-mail address: ito@icrs.tohoku.ac.jp (O. Ito)

1010-6030/00/$ – see front matter
PII: S1010-6030(00)00219-7

by the procedure reported by Gebert et al. [10]. Other chemicals are of the best commercial grade available.

2.2. Apparatus

Time-resolved fluorescence spectra were measured by a single-photon counting method using a second harmonic generation (SHG, 410 nm) of a Ti:sapphire laser (Spectra-Physics, Tsunami 3950-L2S, 1.5 ps FWHM) and a streakscope (Hamamatsu Photonics, C4334-01) as an excitation source and a detector, respectively.

Nanosecond-transient absorption measurements were carried out using third harmonic generation (THG, 355 nm) of an Nd:YAG laser (Spectra-Physics, Quanta-Ray GCR-130, 6 ns FWHM) as an excitation source. For transient absorption spectra in the near-IR region (600–1400 nm), monitoring light from a pulsed Xe-lamp was detected with a Ge-avalanche photodiode (Hamamatsu Photonics, B2834). For the visible region (400–1000 nm), an Si-PIN photodiode (Hamamatsu Photonics, S1722-02) was employed as a detector. Photoinduced events in micro- and millisecond time regions were measured using a continuous Xe-lamp (150 W) and an InGaAs-PIN photodiode (Hamamatsu Photonics, G5125-10) as a probe light and a detector, respectively. Details of the transient absorption measurements have been described in our previous papers [11]. All the samples in quartz cell (1 cm×1 cm) were deaerated by bubbling Ar through the solution for 15 min.

Transient absorption spectra in the picosecond region were measured using the SHG (532 nm) of an active/passive mode-locked Nd:YAG laser (Continuum, PY61C-10, 35 ps FWHM) as an excitation source. Probe light which was generated by breakdown of Xe gas was detected with a streak scope (Hamamatsu Photonics, C2830) and a cooled CCD camera (Hamamatsu Photonics, C4880) after passing through the sample solution.

Steady-state absorption spectra in the visible and near-IR regions were measured on a Jasco V570 DS spectrophotometer.

TEM observation and electron diffraction were carried out using JEOL JEM-2000FX with an accelerating voltage of 200 kV.

Dynamic light scattering (Otsuka Electronics, DLS-7000) was used to estimate the size of the fine particle dispersed in liquid.

3. Results and discussion

3.1. Preparation and ground state properties of C_{60}FP

C_{60}FP was prepared by the reprecipitation method; 0.2 ml CS_2 solution of C_{60} (1 mM) was injected into 10 ml of ethanol under continuous stirring at room temperature. A TEM picture of C_{60}FP shows hexagonal outline and clear lattice fringes inside with 0.8 nm spacing (Fig. 1(a)), which is almost the same with a molecular size of C_{60}, indicating close-packed structure [12]. The close-packed structure of C_{60}FP was supported by the electron diffraction pattern with the hexagonal symmetry coinciding with the face-centered-cubic structure, which results from structure analysis of C_{60} single crystal [13]. The TEM picture (Fig. 1(a)) represents parallel lattice fringes extended from one edge to another without any dislocations. Therefore, it can reasonably be concluded that the C_{60}FP in the present study is a single crystal. Slight disordered structure was formed on the surface, which may play an important role in localization of the excited energy.

From the dynamic light scattering measurement on an ethanol dispersion (Fig. 1(b)), averaged diameter of C_{60}FP was estimated to be 270 nm. While C_{60} solution is purple, C_{60}FP dispersion is light brown, similar to the crystalline color of C_{60}. An absorption spectrum of C_{60}FP dispersed in ethanol showed a peak at 350 nm accompanying shoulders around 450 and 620 nm (Fig. 2). Although the absorption bands are broad, the spectral features of C_{60} are retained. These spectral features rather resemble the C_{60} solid which

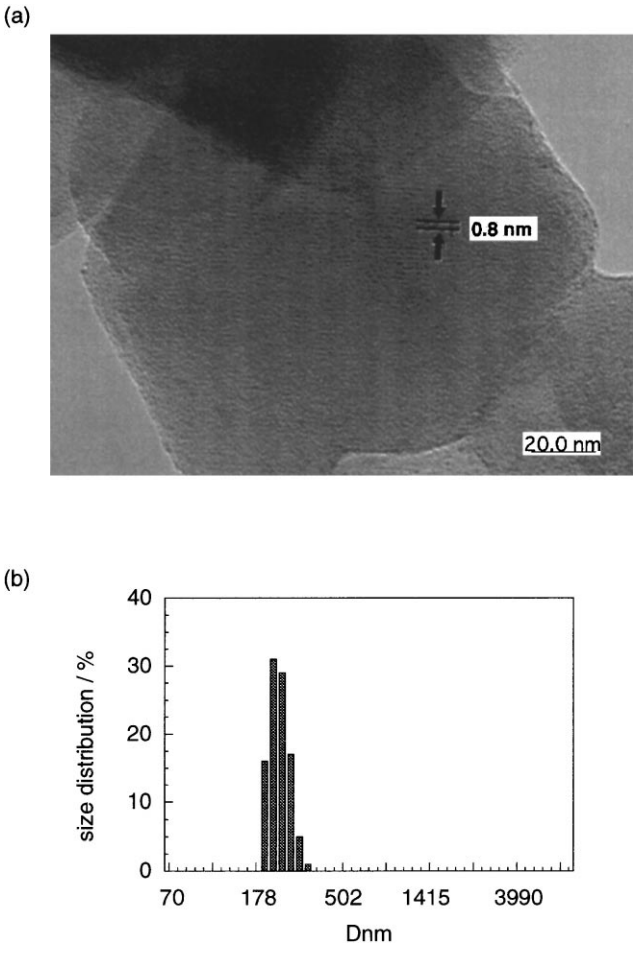

Fig. 1. (a) TEM picture of C_{60}FP. (b) Size distribution of C_{60}FP.

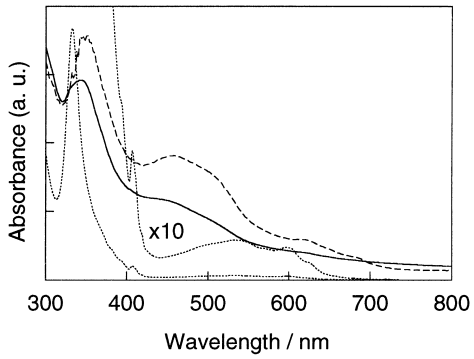

Fig. 2. Absorption spectra of C_{60}FP dispersion in ethanol (solid line), C_{60} solid dispersed in KBr pellet (broken line), and C_{60} in benzene (dot line).

is dispersed in KBr pellet as also shown in Fig. 2, while subtle peak shifts from C_{60} solid are observed.

3.2. Fluorescence property of C_{60}FP

C_{60}FP in ethanol shows fluorescence upon excitation. Its fluorescence band was also broad compared to C_{60} in solution. The peak was observed around 730 nm, which means its peak position is similar to that of C_{60} solution in benzene. The fluorescence decay curve was obtained at 77 K by the single photon counting method as shown in Fig. 3. Fluorescence decay curve can not be analyzed by a single exponential decay function. Energy relaxation mechanism of the singlet-excited state of C_{60} single crystal has been reported by Yang et al. [14]. For the dual fluorescence decay of C_{60} solid, they proposed emission from free exciton and self-trapped exciton, which have been often employed for the excited singlet energy relaxation mechanism of organic crystals (for example [15]). In the present case, fluorescence decay curve of C_{60}FP was analyzed by assuming two components. Curve fitting (solid line in Fig. 3) gives 0.8 and 2.1 ns of lifetimes, which can be attributed to free exciton and self-trapped exciton, respectively. The observed lifetimes are somewhat longer than those reported by Yang et al. for C_{60} solid [14].

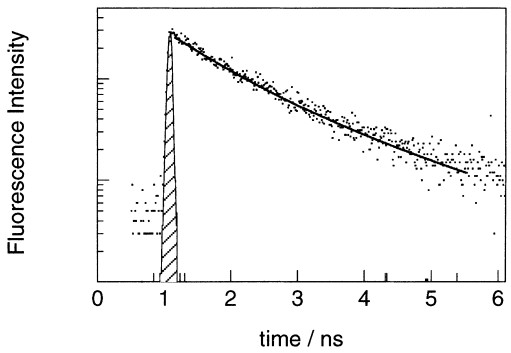

Fig. 3. Fluorescence decay profile around 730 nm of C_{60}FP dispersed in an ethanol/methanol mixture at 77 K. Solid line is the fitted curve.

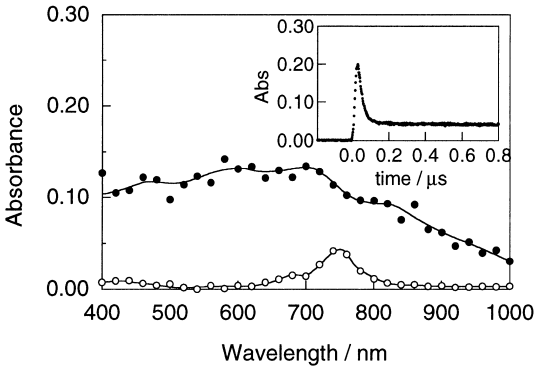

Fig. 4. Transient absorption spectra of C_{60}FP dispersed in ethanol at 50 ns (solid circle) and 500 ns (open circle) after 355 nm laser irradiation. Insert: absorption–time profile at 740 nm.

3.3. Triplet properties of C_{60}FP

The excited state properties of C_{60}FP were also examined by nanosecond-laser flash photolysis. Fig. 4 shows transient absorption spectra of C_{60}FP. Immediately after nanosecond-laser excitation, quite a broad absorption band appeared in the wide region (400–1000 nm) with a peak around 700 nm. As shown in an inset of Fig. 4, the broad absorption decayed within 50 ns, a sharp absorption band remaining at 740 nm, which is similar to that of $^3C_{60}^*$ in solution [16] and can be attributed to the triplet-excited state of C_{60}FP ($^3C_{60}$FP*).

From transient absorption measurements by picosecond-laser flash photolysis (Fig. 5), it was confirmed that the broad absorption band around 700 nm was generated at a rate ($2.0\times10\,s^{-1}$) which is similar to the decay rate of the free exciton ($1.3\times10^9\,s^{-1}$) estimated in Fig. 3. This finding indicates that the broad absorption band around 700 nm is generated by the intersystem crossing process from the singlet-excited state of C_{60}FP. Therefore, the broad absorption band observed in the picosecond-laser photolysis can be attributed to a triplet-excited state of C_{60}FP also, in which $^3C_{60}^*$ interacts with other C_{60} molecules in the C_{60}FP.

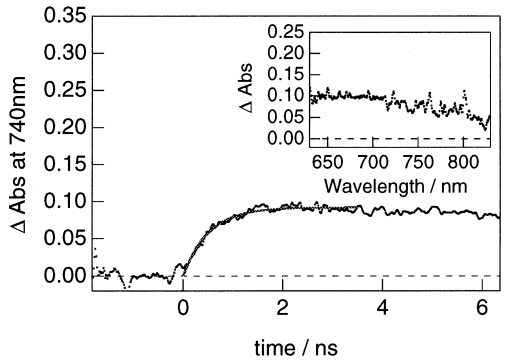

Fig. 5. Absorption–time profile of C_{60}FP dispersed in ethanol at 740 nm after picosecond-laser irradiation at 532 nm. Insert: transient absorption spectrum at 1.4 ns after picosecond-laser irradiation.

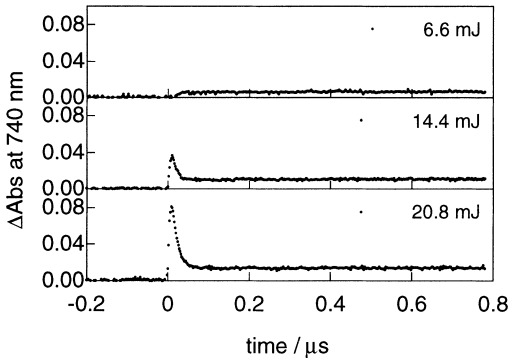

Fig. 6. Excitation laser power dependence of absorption–time profiles of C_{60}FP dispersed in ethanol at 740 nm. Characters show excitation laser power.

In the time profile observed in nanosecond-laser photolysis, the initial absorbance of the broad band largely depended on the excitation laser intensity. The initial broad band could not be observed when the laser power was smaller than 6 mJ per pulse (Fig. 6). Therefore, the fast decay of the broad absorption band is considered to indicate an annihilation of the triplet energy which migrates within C_{60}FP. Applying a second-order plot to the absorption–time profile at 740 nm, $k_{TT}/\varepsilon(({}^3C_{60}^*)_{del})$ was estimated to be 1.2×10 cm s^{-1} where k_{TT} and $\varepsilon(({}^3C_{60}^*)_{del})$ are second-order rate constant of T–T annihilation and extinction coefficient of delocalized ${}^3C_{60}^*$ in C_{60}FP, respectively. Assuming that $\varepsilon(({}^3C_{60}^*)_{del})$ is the same as the extinction coefficient of ${}^3C_{60}^*$ in solution, ($\varepsilon({}^3C_{60}^*)$=16 100 M^{-1} cm^{-1} [17]), 1×10^{14} M^{-1} s^{-1} of k_{TT} was obtained. Based on the same assumption, a fraction of the triplet–triplet annihilation to the initially generated triplet state was estimated to be ca. 0.6 when C_{60}FP was excited by a laser intensity larger than 14 mJ per pulse. After the fast decay, the triplet energy seems to be localized on the C_{60} molecular site as suggested by the sharp peak at 740 nm in Fig. 4. The slow decay component can be analyzed by a first-order decay function and its lifetime was estimated to be 22 μs, which is shorter than that of C_{60} in CS_2 solution (47 μs).

3.4. Energy transfer process

In the presence of oxygen, the transient absorption band due to the localized triplet-excited state was quenched. Since oxygen is a triplet energy quencher, quenching of the localized ${}^3C_{60}FP^*$ (($^3C_{60}FP^*)_{loc}$) can be attributed to an energy transfer process between $({}^3C_{60}FP^*)_{loc}$ and oxygen (Eq. (1)):

$$({}^3C_{60}FP^*)_{loc} + {}^3O_2 \rightarrow C_{60}FP + {}^1O_2^* \quad (1)$$

This finding indicates that $({}^3C_{60}FP^*)_{loc}$ can react with reagent in the solution. In order to confirm the reactivity of $({}^3C_{60}FP^*)_{loc}$ with the reactant in the solution, energy transfer process with β-carotene was attempted, since β-carotene is a good triplet energy acceptor due to its low triplet

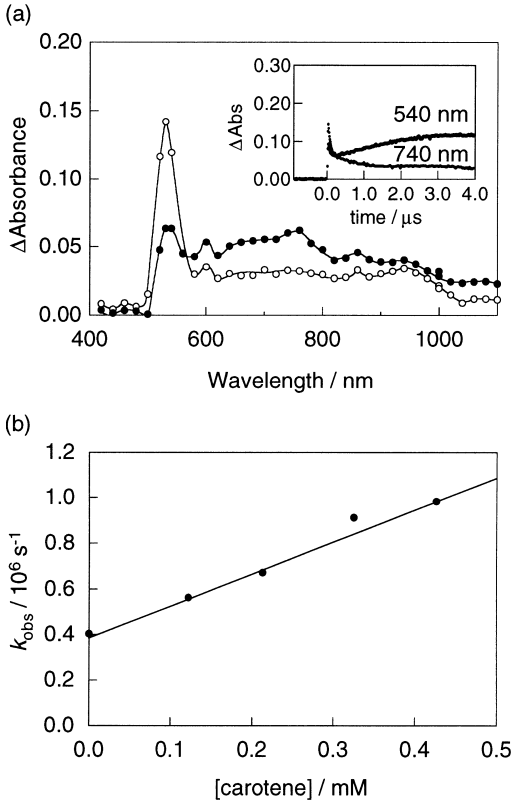

Fig. 7. (a) Transient absorption spectra observed by 355 nm laser irradiation of C_{60}FP in the presence of β-carotene (0.4 mM) in ethanol at 250 ns (solid circle) and 2.5 μs (open circle). Insert: absorption–time profiles at 540 and 740 nm. (b) Dependence of the quenching rate (k_{obs}) of ${}^3C_{60}FP^*$ on concentrations of β-carotene.

energy [18]. Fig. 7(a) shows transient absorption spectra observed by the 355 nm-laser light irradiation of C_{60}FP in the presence of β-carotene in ethanol. At 250 ns after laser irradiation, $({}^3C_{60}FP^*)_{loc}$ is confirmed by an absorption peak at 740 nm. The absorption band of $({}^3C_{60}FP^*)_{loc}$ decayed as shown in the inserted time profiles of Fig. 7(a); a new absorption band appeared at 540 nm which can be assigned to the triplet-excited state of β-carotene in solution [19]. The appearance of ${}^3(\beta\text{-carotene})^*$ with the decay of $({}^3C_{60}FP^*)_{loc}$ supports the following energy transfer process (Eq. (2)):

$$({}^3C_{60}FP^*)_{loc} + \beta\text{-carotene} \xrightarrow{k_{ent}} C_{60}FP + {}^3(\beta\text{-carotene})^* \quad (2)$$

From a dependence of the generation rate of ${}^3(\beta\text{-carotene})^*$ on the concentration of β-carotene (Fig. 7 (b)), an energy transfer rate constant (k_{ent}) can be estimated to be 1.5×10^9 M^{-1} s^{-1} which is somewhat smaller than the diffusion-limiting rate in ethanol ($k_{diff}=5.4\times10$ M^{-1} s^{-1}) [18]. Since pseudo-first-order plot shows a linear line within the examined concentration range of β-carotene, the adsorption of β-carotene on the surface of C_{60}FP may be small.

3.5. Photoinduced reduction of C_{60}FP

C_{60} is known as an excellent electron acceptor in its excited state. In the presence of appropriate electron donors such as aliphatic amines, photoexcitation of C_{60} results in electron transfer from the donors to $^3C_{60}^*$, generating a radical anion of C_{60} ($C_{60}^{\bullet -}$) [20]. Here 1,4-diazabicyclo[2.2.2]octane (DABCO) was employed as an electron donor. The oxidation potential of DABCO is reported to be 0.57 V versus SCE [21] from which a sufficiently negative free energy change ($-47\,kJ\,mol^{-1}$) was evaluated for the electron transfer to $^3C_{60}^*$. It is known that C_{60} and DABCO form a weak 1:1 charge transfer complex in both polar and non-polar solutions [22]. However, the ground state absorption spectrum of ethanol containing C_{60}FP and DABCO was essentially the same as that of C_{60}FP in the examined concentration range of DABCO (5–20 mM). Therefore, the laser light at 355 nm excites C_{60}FP only under the present experimental conditions. Fig. 8 shows transient absorption spectra observed by the 355 nm-laser excitation of C_{60}FP in the presence of 5 mM DABCO in ethanol. The fast decaying part was not changed by the existence of DABCO, because of a fast T–T annihilation process. However, the slowly decaying part at 740 nm was efficiently quenched and a new absorption band appeared at 1080 nm at a similar time scale as shown in the inserted time profile of Fig. 8(a). The latter can be attributed to $C_{60}^{\bullet -}$ [20]. This finding indicates that electron transfer takes place from DABCO to $(^3C_{60}FP^*)_{loc}$ (Eq. (3)). The peak position of the slightly broadened absorption band of $C_{60}^{\bullet -}$ in C_{60}FP is quite similar to that of $C_{60}^{\bullet -}$ in solution, indicating that interaction between $C_{60}^{\bullet -}$ with C_{60} in C_{60}FP is weak.

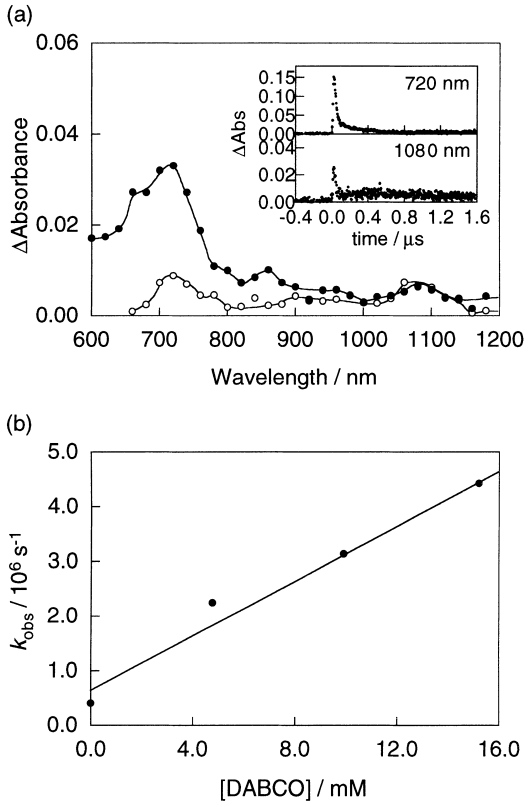

Fig. 8. (a) Transient absorption spectra observed by 355 nm laser irradiation of C_{60}FP in the presence of DABCO (5.0 mM) in ethanol at 100 ns (solid circle) and 500 ns (open circle). Insert: absorption–time profiles at 720 and 1060 nm. (b) Dependence of the quenching rate (k_{obs}) of $^3C_{60}FP^*$ on concentrations of DABCO.

$$(^3C_{60}FP^*)_{loc} + DABCO \xrightarrow{k_{et}} C_{60}FP^{\bullet -} + DABCO^{\bullet +} \quad (3)$$

From dependence of the quenching rates of $(^3C_{60}FP^*)_{loc}$ on the concentration of DABCO (Fig. 8(b)), the bimolecular rate constant of the quenching of $(^3C_{60}FP^*)_{loc}$ was estimated to be $2\times10^8\,M^{-1}\,s^{-1}$, which is smaller than that observed in the electron transfer process between $^3C_{60}^*$ and DABCO in benzonitrile (BN), $4\times10^9\,M^{-1}\,s^{-1}$ [23]. The rate constant for $(^3C_{60}FP^*)_{loc}$ is smaller than the diffusion limit (ethanol $5.4\times10^9\,M^{-1}\,s^{-1}$ [18]), which is reasonable for electron transfer on the surface: since the distribution of $(^3C_{60}FP^*)_{loc}$ will be low due to efficient T–T annihilation, collision frequency between $(^3C_{60}FP^*)_{loc}$ and DABCO is considered to be small. Employing the reported extinction coefficient for $C_{60}^{\bullet -}$ ($12\,100\,M^{-1}\,cm^{-1}$) [24], the yield of the $C_{60}^{\bullet -}$ via $(^3C_{60}FP^*)_{loc}$ was estimated to be 0.4, which is somewhat smaller than the yield of electron transfer between $^3C_{60}^*$ and DABCO in BN, 0.6 [23]. In the present electron transfer between $(^3C_{60}FP^*)_{loc}$ and DABCO, the contribution of DABCO adsorbed on the surface of C_{60}FP is considered to be small, because the reaction with adsorbed molecule should be fast, while the absorption–time profile (insert of Fig. 8(a)) did not show any sign of fast electron transfer reaction. Furthermore, a linear pseudo-first-order plot indicates that the electron transfer with DABCO adsorbed on the surface of C_{60}FP may be small.

3.6. Photoinduced oxidation of C_{60}FP

Nonell et al. reported that the radical cation of C_{60} ($C_{60}^{\bullet +}$) can be generated in a high yield by the photosensitized electron transfer process using a cosensitizer in solution [25]. For example, using NMA^+ and biphenyl (BP) as a sensitizer and a cosensitizer, respectively, $C_{60}^{\bullet +}$ was generated by following reaction schemes (Eqs. (4) and (5)):

$$NMA^+ \xrightarrow{h\nu} {}^SNMA^+ \xrightarrow{BP} NMA^{\bullet} + BP^{\bullet +} \quad (4)$$

$$BP^{\bullet +} + C_{60} \rightarrow BP + C_{60}^{\bullet +} \quad (5)$$

Recently, we reported that the same oxidation is also applicable to other fullerenes such as C_{70}, C_{76}, and C_{82} [26,27]. Here, C_{60}FP was examined to donate an electron to $BP^{\bullet +}$ in this reaction system. Immediately after the 355 nm-laser excitation which excites NMA^+ mainly, a transient absorption band appeared at 980 nm which can be attributed to the radical cation of C_{60}FP from comparison with the spectrum

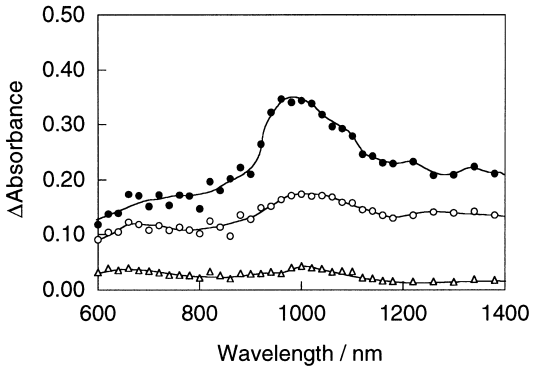

Fig. 9. Transient absorption spectra observed by 355 nm laser irradiation of C_{60}FP in the presence of NMA^+ (0.2 mM) and biphenyl (200 mM) in ethanol at 100 ns (solid circle), 200 ns (open circle), and 1 μs (open triangle).

reported for the radical cation of C_{60} (Fig. 9) [25]. This finding indicates that C_{60} on the surface of C_{60}FP has high reactivity to $BP^{\bullet+}$ in solution.

It is worth mentioning that the observed absorption bands due to the triplet-excited state, radical cation, and radical anion of C_{60}FP are located at quite close to those reported for isolated C_{60} in solution. These findings indicate that the electronic structures of these transient species are not strongly affected by crystalline structure as often discussed for the organic molecular crystals [28].

4. Conclusion

In the present paper, we examined the photophysical and photochemical properties of C_{60}FP. Relaxation processes such as fluorescence decay and T–T annihilation were quite different from those reported for isolated C_{60} in solution, since these events are mainly ruled by crystalline structure. On the other hand, photoinduced processes of the localized triplet state such as energy transfer and electron transfer were observed as in the case of isolated C_{60} in solution, while the reaction rates were small due to low collision frequency of $(^3C_{60}FP^*)_{loc}$. In this sense, the fine particle is considered to be an interesting research field for photochemical investigation.

Acknowledgements

The present work is partly supported by the Grant-in Aid on Scientific Research on Priority Area (B) on ‘Laser Chemistry of Single Nanometer Organic Particle’ (No. 10207202) from the Ministry of Education, Science, Sports, and Culture, Japan.

References

[1] M.L. Steigerwald, L.E. Brus, Acc. Chem. Res. 23 (1990) 183.
[2] E. Hanamura, Phys. Rev. B 37 (1988) 1273.
[3] H. Kasai, H.S. Nalwa, H. Oikawa, S. Okada, H. Matsuda, N. Minami, A. Kakuta, K. Ono, A. Mukoh, H. Nakanishi, Jpn. J. Appl. Phys. 31 (1992) L1132.
[4] M. Fujitsuka, H. Kasai, A. Masuhara, S. Okada, H. Oikawa, H. Nakanishi, A. Watanabe, O. Ito, Chem. Lett. (1997) 1211.
[5] H. Toyotama, Kinouzairyo (Functional Materials) 6 (1987) 44.
[6] K. Yase, T. Inoue, M. Okada, T. Funada, J. Hirano, Hyomen-Kagaku (Surface Science) 8 (1989) 434.
[7] Y.P. Sun, C.E. Bunker, Nature 365 (1993) 398.
[8] H.N. Ghosh, A.V. Sapre, J.P. Mittal, J. Phys. Chem. 100 (1996) 9439.
[9] S. Nath, H. Pal, D.K. Palit, A.V. Sapre, J.P. Mittal, J. Phys. Chem. B 102 (1998) 10158.
[10] H. Gebert, W. Regenstein, J. Bendig, D. Kreysig, Z. Phys. Chem. 263 (1982) 65.
[11] M. Fujitsuka, A. Watanabe, O. Ito, K. Yamamoto, H. Funasaka, J. Phys. Chem. A 101 (1997) 4840.
[12] K. Yase, T. Hanada, H. Kasai, T. Sato, S. Okada, H. Oikawa, H. Nakanishi, Mol. Cryst. Liq. Cryst. 294 (1997) 71.
[13] P.A. Heiney, J.E. Fischer, A.R. McGhie, W.J. Ramanow, A.M. Denestein, J.P. McCauly Jr, A.B. Smith III, Phys. Rev. Lett. 66 (1991) 2911.
[14] S.I. Yang, Y.D. Suh, S.M. Jin, S.K. Kim, J. Park, E. Shin, D. Kim, J. Phys. Chem. 100 (1996) 9223.
[15] H. Nishimura, T. Yamaoka, K. Mizuno, M. Iemura, A. Matsui, J. Phys. Soc. Jpn. 53 (1984) 3999.
[16] R.J. Sension, C.M. Phillips, A.Z. Szarka, W.J. Romanow, A.R. McGhie, J.P. McCauley Jr., A.B. Smith III, R.M. Hochstrasser, J. Phys. Chem. 95 (1991) 6075.
[17] N.M. Dimitrijevic, P.V. Kamat, J. Phys. Chem. 96 (1992) 4811.
[18] S.L. Murov, I. Carmichael, G.L. Hug, Handbook of Photochemistry, 2nd Edition, Marcel Dekker, New York, 1993.
[19] I. Carmichael, G.L. Hug, J. Phys. Chem. Ref. Data 15 (1986) 1.
[20] J.W. Arbogast, C.S. Foote, M. Kao, J. Am. Chem. Soc. 114 (1992) 2277.
[21] G.J. Kavarnos, N.J. Turro, Chem. Rev. 86 (1986) 401.
[22] K.I. Priyadarsini, H. Mohan, A.K. Tyagi, J.P. Mittal, Chem. Phys. Lett. 230 (1994) 317.
[23] A. Masuhara, M. Fujitsuka, O. Ito, submitted for publication.
[24] H.A. Heath, J.E. McGrady, R.L. Martin, J. Chem. Soc., Chem. Commun. (1992) 1272.
[25] S. Nonell, J.W. Arbogast, C.S. Foote, J. Phys. Chem. 96 (1992) 4169.
[26] M. Fujitsuka, A. Watanabe, O. Ito, K. Yamamoto, H. Funasaka, J. Phys. Chem. A 101 (1997) 7960.
[27] M. Fujitsuka, A. Watanabe, O. Ito, K. Yamamoto, H. Funasaka, T. Akasaka, J. Phys. Chem. B 103 (1999) 9519.
[28] M. Pope, C.E. Swenberg, Electronic Processes in Organic Crystals, Clarendon Press, Oxford, 1982.